1 **Tissue-enhanced plasma proteomic analysis for disease stratification in**

2 **amyotrophic lateral sclerosis**

3 **Irene Zubiri[1,2], Vittoria Lombardi[1], Michael Bremang[2], Vikram Mitra[2], Giovanni**

4 **Nardo[3], Rocco Adiutori[1] , Ching-Hua Lu[1,5], Emanuela Leoni[1,2] , Ping Yip[1], Ozlem Yildiz[1],**

5 **Malcolm Ward[2] , Linda Greensmith[4], Caterina Bendotti[3], Ian Pike[2], Andrea Malaspina[1].**

6 1. Neuroscience and Trauma Centre, Blizard Institute, Barts and The School of Medicine and

7 Dentistry, Queen Mary University of London, London, United Kingdom.

8 2. Proteome Sciences plc, Hamilton House, Mabledon Place, London, United Kingdom.

9 3. Laboratory of Molecular Neurobiology, Department of Neuroscience, IRCCS - Istituto di

10 Ricerche Farmacologiche Mario Negri, Milan, Italy.

11 4. Sobell Department of Motor Neuroscience and Movement Disorders, MRC Centre for

12 Neuromuscular Disorders, UCL Institute of Neurology, University College London, London,

13 United Kingdom.

14 5. Department of Neurology, China Medical University Hospital, Taichung City, Taiwan.

15 **Corresponding authors:** Andrea Malaspina and Irene Zubiri. Neuroscience and Trauma
16 Centre, Blizard Institute, Barts and The School of Medicine and Dentistry, Queen Mary
17 University of London, 4 Newark Street, London, City of London, Greater London E1 2AT.
18 Email address irenezubiri@gmail.com. Telephone: 0207 882 2283. Andrea Malaspina.
19 Neuroscience and Trauma Centre, Blizard Institute, Barts and The School of Medicine and
20 Dentistry, Queen Mary University of London, 4 Newark Street, London, City of London,
21 Greater London E1 2AT. Email address: a.malaspina@qmul.ac.uk Telephone: 0207 882 6239.

22 **ABSTRACT**
23
24 **Background:**

25 It is unclear to what extent pre-clinical studies in genetically homogeneous animal models of
26 amyotrophic lateral sclerosis (ALS), an invariably fatal neurodegenerative disorder, can be
27 informative of human pathology. The disease modifying effects in animal models of most
28 therapeutic compounds have not been reproduced in patients. To advance therapeutics in ALS,
29 we need easily accessible disease biomarkers which can discriminate across the phenotypic
30 variants observed in ALS patients and can bridge animal and human pathology. Peripheral
31 blood mononuclear cells alterations reflect the rate of progression of the disease representing
32 an ideal biological substrate for biomarkers discovery.

33 **Methods:** We have applied TMTcalibrator™, a novel tissue-enhanced bio fluid mass
34 spectrometry technique, to study the plasma proteome in ALS, using peripheral blood
35 mononuclear cells as tissue calibrator. We have tested slow and fast progressing SOD1G93A
36 mouse models of ALS at a pre-symptomatic and symptomatic stage in parallel with fast and
37 slow progressing ALS patients at an early and late stage of the disease. Immunoassays were
38 used to retest the expression of relevant protein candidates.

Results: The biological features differentiating fast from slow progressing mouse model plasma proteomes were different from those identified in human pathology, with only processes encompassing membrane trafficking with translocation of GLUT4, innate immunity, acute phase response and cytoskeleton organization showing enrichment in both species. Biological processes associated with senescence, RNA processing, cell stress and metabolism, major histocompatibility complex-II linked immune-reactivity and apoptosis (early stage) were enriched specifically in fast progressing ALS patients. Immunodetection confirmed regulation of the immunosenescence markers Galectin-3, Integrin beta 3 and Transforming growth factor beta-1 in plasma from pre-symptomatic and symptomatic transgenic animals while Apolipoprotein E differential plasma expression provided a good separation between fast and slow progressing ALS patients.

Conclusions: These findings implicate immunosenescence and metabolism as novel targets for biomarkers and therapeutic discovery and suggest immunomodulation as an early intervention. The variance observed in the plasma proteomes may depend on different biological patterns of disease progression in human and animal model.

Key Words

Amyotrophic lateral sclerosis, proteomics, biomarkers, TMTcalibrator™, SOD1G93A animal models.

BACKGROUND

Amyotrophic lateral sclerosis (ALS), a fatal neurodegenerative disorder, is a clinically heterogeneous condition where survival can be less than a year or more than a decade from symptoms onset, making any assessment of treatment response in clinical trials difficult in absence of reliable estimates of prognosis [1]. A significant diagnostic delay in ALS prevents

63 early treatment reducing the prospect of therapeutic success [2]. Mutant superoxide dismutase
64 1 (SOD1G93A) transgenic mice models of ALS are widely used as surrogates of human
65 pathology in pre-clinical research. A relatively uniform genetic background and the strictly
66 controlled environmental and breeding conditions make SOD1G93A transgenic animals ideal
67 models to investigate the disease pathobiology and the pre-symptomatic disease stage [3, 4].
68
69 Experimental evidence suggests that the rate of disease progression in ALS may be linked to
70 the immunological response to neuronal degeneration, which is reproduced systemically by
71 altered blood levels of cytokines, acute phase reactants and by an early down-regulation of
72 FoxP3-positive T regulatory cells predominantly in patients with a faster disease progression
73 [5, 6]. In SOD1G93A transgenic mouse models of ALS, symptomatic disease can develop
74 with a slow and fast progression in C57 and 129Sv genetic backgrounds respectively (here
75 defined as Sym-SOD1C57 and Sym-SOD1129S). In these SOD1G93A transgenic mice,
76 impairment of the protein quality control in the spinal cord and the activation of the major
77 histocompatibility complex I (MHCI) expression in axons and neuromuscular junctions are
78 considered indices of fast disease progression [7, 8].
79
80 The inflammatory response in ALS co-exists with a state of deranged lipid metabolism and
81 altered total daily energy expenditure [6, 9, 10], associated also with the effects of genetic
82 mutations of the TDP-43 and C9orf72 genes linked to familial ALS [11-14]. Importantly, it is
83 also acknowledged that functionally competent and high energy-demanding motor neurons
84 are vulnerable to chronic inflammation and changes in metabolism [15-17] while aging, one
85 of the main risk factors for ALS, may increase neuronal vulnerability with a decline in cell
86 glucose uptake and mitochondrial energy production [18].
87

88 Over 50 randomized controlled clinical trials in ALS have been unsuccessful, despite many
89 compounds having shown a disease-modifying effect in animal models [19-21]. There is
90 therefore a critical need to improve translation of pre-clinical results into clinical trial
91 outcomes in ALS, through the identification of molecular factors driving disease progression
92 in humans and rodents which can be used for phenotypic stratification across species. To this
93 end, a viable strategy is the molecular profiling of accessible biofluids and of Peripheral
94 Blood Mononuclear Cells (PBMC), central to many aspects of the systemic immunological
95 reaction to neurodegeneration [22, 23]. TMTcalibrator™, an unbiased proteomics method, is
96 ideally placed to combine tissue and fluid proteomics in a single experiment, providing
97 significant gains in sensitivity and a direct link between protein expression in diseased tissue
98 and in matched fluids [24].
99
100 In this study, we have used TMTcalibrator™ to investigate biological features which are
101 regulated in plasma and are also coherently expressed in matched PBMC samples from
102 pre-symptomatic and symptomatic SOD1G93A transgenic mouse models of ALS with a fast
103 (129Sv strain) and a slow (C57 strain) progression of the disease. We have used the same
104 approach to test the plasma/PBMC proteome in fast and slow progressing ALS patients
105 (defined as ALS-Fast and ALS-Slow), at an early and late stage of the disease. We have
106 detected an early inflammatory and acute phase response in both human and animal model,
107 while perturbed metabolism and an overall switch to cellular senescence is seen in fast
108 progressing human pathology. We found only a partial overlap of the plasma/PBMC
109 proteome between rodents and humans, suggesting a variability which is disease-stage
110 dependent.
111

112 # METHODS

113 **Animal models**

114 Female superoxide dismutase 1 (SOD1) transgenic mice with a G93A mutation in a
115 C57BL/6JOlaHsd (C57SOD1G93A) and in a 129SvHsd (129SvSOD1G93A) genetic
116 background and wild-type female littermates (defined as WTC57 and WT129Sv) were used in
117 this study (Jackson Laboratories, B6SJL-TgNSOD-1-SOD1G93A-1Gur). The development of
118 the symptomatic stage of the disease differed significantly in the two SOD1G93A transgenic
119 mouse strains, with regards to disease onset and duration [8, 25]. In this study, fast developing
120 symptomatic SOD1G93A transgenic mice are defined as Sym-SOD1129Sv (129Sv pre-
121 symptomatic mice as Pre-SOD1129Sv), while slow symptomatic progressing mice as Sym-
122 SOD1C57 (C57 pre-symptomatic mice as Pre-SOD1C57). SOD1G93A transgenic animals
123 expressed 20 copies of the human Gly93Ala SOD1 gene substitution in the C57OlaHsd and
124 129SvHsd backgrounds for more than 30 and 10 generations respectively. Mice were
125 maintained in a specific pathogen-free environment (21°C temperature, 10% relative humidity
126 in a 12 hour of light/dark cycle) with food/water supplied ad libitum and adaptations for
127 animals with a substantial motor impairment. Mice of both strains were considered in a
128 symptomatic stage when they exhibited a 50% decrease in latency of grip strength and a 45%
129 body weight decline from the peak values in the pre-symptomatic stage [26]. Plasma samples
130 from Wild type (WT) animals used in the re-test experiments were obtained at the same time
131 of blood collection from both pre-symptomatic and symptomatic SOD1G93A transgenic
132 animal models.

133

134 **Patient selection**

135 ALS patients and biological samples were selected from the ALS biomarkers study
136 biorepository (Ethical approval: London and the City Research Ethics Committee 1
137 09/H0703/27). Exclusion criteria were neuroinflammatory and neurodegenerative

comorbidities, recent mechanical injuries and/or infections, systemic autoimmune disorders, cancer, pro-thrombotic states, family history of ALS or frontotemporal dementia (FTD) as well as known genetic mutation linked to ALS or FTD. The Functional Rating Scale-Revised (ALSFRS-R; range 1 to 48, with increasing levels of neurological impairment with lower scores) was used to define the level of neurological impairment, with early ALS corresponding to a score > 40 and late ALS < 35. Disease progression to last visit (PRL) was calculated as "48 - ALSFRS-R at the last visit, divided for disease duration from onset to the last visit in months" (fast ALS progression: $PRL>0.7$; slow ALS progression: $PRL< 0.5$)[6] .

Sample collection, plasma and mononuclear cell extraction and processing

18 ml blood were collected in EDTA tubes and centrifuged at 800g for 10 minutes at room temperature. Plasma was recovered and centrifuged at 3500rpm for 10 minutes and stored at -80°C. Plasma samples were albumin and IgG depleted (ProteoPrep® Immunoaffinity kit). PBMC were isolated by density-gradient 2,000 rpm centrifugation for 40 minutes at 20°C using Lymphoprep™ (Alere) and subsequently washed in Dulbecco's phosphate-buffered saline (Gibco). PBMC pellets were stored at -80°C in a freezing solution (10% DMSO in foetal bovine serum). After 24 hours, PBMC aliquots were transferred into liquid nitrogen. PBMC samples were thawed at 37°C and re-suspended in 10 ml warm (37°C) Dulbecco phosphate buffer. Cell suspension was centrifuged at room temperature and the pellet was re-suspended in 100 µl of lysis buffer (8 M urea, 75 mM NaCl, 50 mM Tris, pH 8.2, protease inhibitors cocktail, cOmplete™, Mini Protease Inhibitor Co, Sigma). Blood was collected from mice cheek and diluted in 3 ml medium (2.5 mM EDTA, 2% FBS in PBS) for PBMC and plasma fractions isolation as reported above. PBMC samples were lysed, sonicated and stored at -80° C.

162

163 **In-Solution Tryptic Digest, Tandem mass tag (TMT®) labelling and TMT**
164 **calibrator™**

165 Protein quantification was carried out using a Bradford Protein Assay (Bio Rad). 100 µg (30
166 µg for mice) protein from depleted plasma and 1 mg (750 µg for mice) from the PBMC pool
167 were dried down in a vacuum centrifuge (SpeedVac, Thermo Scientific). Following
168 solubilisation and denaturation in 100 mM Triethylammonium bicarbonate (TEAB)/0.1%
169 (w/v) SDS), samples were reduced with 1 mM tris (2-carboxyethyl) phosphine 10 (TCEP) at
170 55 °C for 60 minutes and alkylated with 7.5mM iodoacetamide at room temperature (RT) for
171 60 minutes. Trypsin (MS grade, Promega) was added at a 1:25 (w/w) ratio to total protein and
172 incubated at 37°C overnight. Digestion products were labelled with TMT®10plex reagents
173 (Thermo Scientific) and incubated at RT for 60 minutes. Six of the 10 isobaric TMT® reagents
174 were used to label individual plasma samples and the total amount of PBMC protein pool was
175 divided among the remaining 4 TMT channels (the four-point calibrator) comprising 1/21,
176 4/21, 6/21 and 10/21 total protein respectively. To quench the TMT® reaction, 0.25%
177 hydroxylamine was added. The samples were then combined to form the analytical 10plex sets,
178 desalted in RP18 columns and dried under vacuum. The human plasma samples were divided
179 into four TMT®10plex sets, two for the early and two for the late time point plasma samples.
180 Each set contained three ALS-Fast and three ALS-Slow plasma samples in combination with
181 the four-point PBMC pool lysate, used as calibrator. The same experimental design was applied
182 to the animal model study, where four different TMT®10plex sets were used to compare 24
183 samples in total. Two TMT®10plex sets included samples from transgenic mice, one for Pre-
184 SOD1129Sv and Pre-SOD1C57, and the other one for Sym-SOD1129Sv and Sym-SOD1C57
185 (n=3 for each genetic background plus 4 channels in each set for the PBMC calibrator). The

186 remaining two TMT®10plex sets included plasma samples from the equivalent Wild type (WT)
187 animals for both 129Sv and C57genetic backgrounds (n:3 per group), collected at the same
188 time blood was taken from pre-symptomatic and symptomatic animal (additional file 2,
189 supplementary fig 1 A, shows sample distribution across TMT®10plexes).

190

191 **Strong Cation exchange (SCX) Fractionation and liquid chromatography tandem**
192 **mass spectrometry (LC-MS/MS)**

193 Each analytical 10plex sample was reconstituted and loaded onto a Polysulfoethyl-A column
194 (4.6 × 100mm, 5 µm, 200 Å, PolyLC) attached to a Waters 2695 HPLC. Quantitative analysis
195 was performed using an Orbitrap Fusion™ Tribrid™ mass spectrometer in positive ion mode
196 with an EASY nLC1000 system and 50cm EASY-Spray column (all Thermo Scientific). More
197 details on the SCX and LC-MS/MS methodologies are reported in the additional file 1.

198

199 **Mass spectrometry analysis and computational proteomics**

200 All plasma samples and pooled PBMC lysates used as tissue calibrator passed sample quality
201 control protocols (data not shown) and were divided into four TMT®10plex sets. All mass
202 spectrometry files were inspected independently and passed internal quality control metrics
203 (data not shown). Outputs of computational proteomics from the 40 raw data files from each
204 TMT®10plex study (human and animal model study) were assembled into a single dataset and
205 processed by Proteome Sciences' proprietary workflows for TMTcalibrator™ including data
206 integration (CalDIT), pre-processing and feature selection (FeaST). Normalised quantitative
207 data were provided for all plasma peptides channels as a ratio against the calculated mid-point

208 value of the PBMC calibrator channels (see additional file 2, supplementary figure 1 describing
209 the experimental workflow).

210 Peptide identification and quantification

211 For each experiment, raw mass spectrometry data files were submitted to Proteome Discoverer
212 (PD) v1.4 (Thermo Scientific), using the Spectrum Files node. The spectrum selector was set
213 to its default values while the SEQUEST-HT node was set to search data against the human or
214 mouse (supplemented with the human SOD1 sequence) FASTA UniProtKB and Swiss-Prot
215 database respectively. A more detailed description of the peptide identification and
216 quantification process is reported in additional file 1.
217

218 Data assembly, pre-processing and normalisation

219 In the first step of the CalDIT workflow, reporter ion intensities were corrected to remove the
220 contribution of signals from adjacent reporter ion channels. Subsequently, within each mass
221 spectrometry run, intensity values across the four calibrant channels (129C, 130N, 130C, 131)
222 were normalised (median-scaling) and, for each peptide spectrum match (PSM), a reference
223 intensity value was calculated based on the calibrant intensity distribution. This reference value
224 was then used to calculate Log_2-transformed PSM ratio values for each of the experimental
225 channels, resulting in lower variance between PSM-level quantifications of the same peptide
226 sequence at different points of the elution profile, or MS runs. To generate peptide expression
227 (ratio) values, median values were then computed across quantified PSMs of the same peptide
228 sequence.
229 In the first step of the FeaST workflow, peptides with more than ~ 35% missing quantitative
230 values within an experimental group (*i.e.* ALS-Fast-Early; ALS-Fast-Late; ALS-Slow-Early;
231 ALS-Slow-Late) were removed from subsequent analysis. Remaining peptides, with values

232 below the percentage threshold, were replaced by values imputed using the k-nearest
233 neighbours (n=2) imputation method, applied to samples within each experimental group. In
234 order to reduce the batch effect created by the use of multiple TMT®10 plexes, a LIMMA-
235 based batch effect correction procedure was applied (additional file 2, supplementary figure 2),
236 using a linear model constructed on the TMT® 10plex batch number and TMT® channel and
237 specifying the experimental groups (PCA before batch effect correction additional file 2,
238 supplementary figure 2). For protein-level analysis, the same procedure was applied in a
239 parallel analysis and, subsequently, expression values were computed by averaging (trimmed
240 mean, trim factor: 0.2) ratios of all non-phosphorylated peptides which matched uniquely to
241 the gene identifier.
242
243 Two quality control metrics per sample were calculated: the median (measure of central
244 tendency) and the inter-quartile range (IQR), measure of scale, using peptide and protein
245 distributions. A sample was considered as a strong outlier if either QC metric value was more
246 than three standard deviations from the overall mean.
247

248 **Immunoassays**

249 Expression analysis of 5 protein candidates in mouse and human plasma samples was
250 undertaken by enzyme-linked immunosorbent assay (ELISA) using commercial kits, a
251 electrochemiluminescence (ECL)-based Meso Scale Discovery (MSD) platform and by
252 Western blot. Plasma samples were processed, aliquoted and frozen at -80°C within 1 hour
253 from blood collection, according to standard consensus procedures. ECL-MSD was used to
254 quantify Apolipoprotein E (APOE; R-PLEX Antibody Set F212I), Galectine-3 (R-PLEX
255 Antibody Set F214F) and transforming growth factor beta-1 (TGFB1; U-PLEX kit

256 K151XWK), in human and mouse plasma, and Apolipoprotein A1 (ApoA1; R-PLEX Antibody
257 Set F21PR) in human. A commercial ELISA was used to analyse ITGB3 and Apo A1 in mouse
258 plasma (Biorbyt orb408222 and Abbexa abx254777 respectively) as well ITGB3 in human
259 plasma (Biorbyt orb407522). Standards, primary and secondary antibodies, detection range
260 including lower and upper limits of detection were specified in the manufacturer's conditions.
261 Plasma samples from Wild-type (WT) and SOD1G93A transgenic mice (both pre-symptomatic
262 and symptomatic), from ALS-Fast, ALS-Slow and healthy controls were equally distributed
263 on each plate and measured in duplicate. Each plate contained a target-specific calibrator:
264 APOA1 (0-1,000,000pg/ml for human and 7.81-500ng/ml for mouse); APOE (0-
265 200,000pg/ml); Galectin-3 (03,000pg/ml), TGFB1 (0-56,600pg/ml) and ITGB3 (125-8000
266 pg/ml for human 62.5-4000pg/ml for mice).

267 For Western blot analysis of ITGB3, 40 µg of albumin-depleted proteins were diluted in
268 Laemmli buffer and loaded onto 10% acrylamide gels. After electrophoresis, proteins were
269 transferred onto nitrocellulose membranes and blocked with Tris buffered saline 0.1% Tween
270 (TBS-T) containing 5% non-fat dry milk powder and -20 for 1h at room temperature.
271 Membranes were then incubated overnight with rabbit anti-Integrin β3 antibody 1:1000
272 (Integrin β3, D7X3P XP® Rabbit mAb #13166. Cell Signaling Technology, Inc.) and with
273 anti-Galectin-3 antibody (Mouse monoclonal Galectin 3 ab2785, Abcam Ltd.) in TBS-T
274 (0.1%) containing 5% bovine serum albumin (BSA) and further incubated with horseradish
275 peroxidase (HRP)-conjugated swine anti-rabbit 1:2500 (Dako) as secondary antibody in TBS-
276 T (0.1%) containing 5% BSA. Enhanced chemiluminescence (ECL kit; GE Healthcare), the
277 ChemiDoc XRS+ imaging system and the image lab 5.2.1 (Bio-Rad) software were used for
278 signal detection acquisition and analysis.

279

280 **Statistical analysis and data mining**

281 All statistical methods applied for the proteomic data analysis were performed using an in-
282 house workflow called FeaST, developed in R statistical programming environment. Principal
283 component analysis (PCA) score and loading plots were generated to study the variance
284 structure of the data sets, indicating technical and biological factors and the influence of each
285 step in the data pre-processing and normalisation workflow. Multifactorial linear modelling
286 (LIMMA) was applied to determine significantly regulated features (peptides or proteins),
287 using the following linear model: logRatio ~ Class + Age + Stage + Group (ALS/Control).
288 Log_2 fold changes (logFC) and p-values were calculated for all peptides and proteins that
289 passed the filtering criteria described (above). The significance criterion α was standardly set
290 to 0.05 to consider a feature as "regulated". Multiple testing was performed using a Benjamini-
291 Hochberg correction.
292
293 Proteome Sciences' proprietary workflows for functional analysis (FAT) were used to identify
294 differences among phenotypic variants in biological processes extracted from plasma
295 proteomes. Significance of *enrichment* was evaluated based on the results of Fisher's Exact
296 Test and multiple test corrections were applied (Benjamini-Hochberg). Functional terms used
297 in this analysis included Gene Ontology Biological Processes and Reactome Pathways. Human
298 and mouse-specific annotations were extracted from publicly-available data repositories. A
299 minimum of two matched gene names was required and terms were considered significant. for
300 a 3-group comparison.
301
302 For the immunoassay data, statistical analysis was performed using GraphPad Prism 6.
303 Continuous variables were presented in median (interquartile range) and nonparametric
304 analysis for group comparisons (with Dunn's multiple comparisons test) as well as correlation

305 analysis were applied. We used log rank analysis (Mantel-Cox test) to compare survival (fixed
306 date was used to censor data for survival analysis). Receiver operating characteristic curve
307 analysis was used to assess assay sensitivity/specificity and diagnostic performance. A *p* value
308 of less than 0.05 was considered statistically significant.
309
310 We have used a RNA-Seq transcriptome and splicing database of glia, neurons and vascular
311 cells of the cerebral cortex to look at cell type-specific expression in the central nervous system
312 (CNS) of Galectin-3, TGFb1 and ITGB3
313 (https://web.stanford.edu/group/barres_lab/brain_rnaseq.html).
314

315 # RESULTS

316 ## Patients and controls

317 17 patients with a diagnosis of possible, probable, laboratory-supported and definite ALS
318 according to the El Escorial criteria [27] were enrolled in the discovery study (demographic
319 and clinical features reported in Table 1A, B). Plasma samples from 12 of these, including six
320 ALS-Fast (progression rate to last visit (PRL) >0.7; male/female ratio 3/3, average age at
321 disease onset 61.7, 48-67; average disease duration to death or last visit 20.5 months (11-32))
322 and six with a slow rate of progression (PRL<0.5; 5 male/1 female, average age at disease onset
323 58.1, 35-71; average disease duration to death or last visit 107 months (97, 254)) were included
324 in the exploratory proteomics as analytical samples, while PBMC samples isolated from blood
325 donated by the remaining five patients were used in the tissue calibrant channels (PRL range:
326 0.023 – 2.5; three male / two female, average age at disease onset 65.8, 57-68), Table 1).
327
328 Blood samples from an additional cohort of 47 ALS patients, including 24 ALS-Fast and 23
329 ALS-Slow, and 29 healthy age and gender-matched controls were used to re-test plasma

330 expression of selected protein candidates using immunodetection. The average age of disease
331 onset among the ALS sub-groups was comparable to the average age of sampling in the healthy
332 control group (Table 1). The most common genetic mutations linked to familial ALS were
333 excluded and all ALS patients had plasma CRP and ferritin levels within normal limits at the
334 time of sampling (normal values: CRP < 5 mg/L; ferritin 10 - 160 μg/L) [6].
335
336
337
338

339

A. DISCOVERY EXPERIMENT: ALS PLASMA SAMPLES

ALS type	**ALSFRS -R** early	**ALSFRS-R** late	**Gender** M/F	**Age at onset** (years)	**PRL**	**Time from onset to death or last visit** (months)	**Time from onset to first sample** (months)	**Time between first and last sample** (months)	**Site of disease onset** limb/ bubar
Slow (n:6)	43 (41- 45)	31.5 (27-35)	5M / 1F	58.1 (35-71)	0.25 (0.1 – 0.4)	107 (97, 254)	76 (30-192)	58 (48-69)	4 limb /2 bulbar
Fast (n:6)	43.8 (41-46)	28.6 (22-35)	3M / 3F	61.3 (48-67)	1.5 (1-1.9)	20.5 (11-32)	10.2 (5-19)	13.8 (7-22)	3 limb /3 bulbar

B. DISCOVERY EXPERIMENT: ALS PBMC SAMPLE TO FORM THE REFERENCE POOL

ALS Pool	**ALSRS-R**	**Gender** M/F	**Age at onset** (years)	**PRL**	**Time from onset to death or last visit** (months)	**Time from onset to sampling (months)**	**Site of disease onset** limb/ bubar
Slow(3) *Fast* (2) n:5	31 (22-42)	3M /2 F	65.8 (57-68)	0.8 (0.02–2.5)	64.6 (8-120)	19 (7 – 44)	3 limb /2 bulbar

C. RE-TEST EXPERIMENT: ALS PLASMA SAMPLES

ALS type	**ALSRS-R**	**Gender** M/F	**Age at onset** (years)	**PRL**	**Time from onset to death or last visit** (months)	**Time from onset to sampling (months)**	**Site of disease onset limb/ bubar**
Slow (n: 23)	39 (18-47)	18M / 5F	65.25 (37-86.9)	0.216 (0.03 – 0.47)	120.4 (28-335.2)	62.8 (7 -248.8)	15 limb /8 bulbar
Fast (n: 24)	33 (13-43)	8M / 16F	62.8 (34.8-82.4)	1.48 (0.74 – 3.6)	28.1 (5 – 50)	14.8 (2.8 – 29.8)	13 limb /11 bulbar

D. RE-TEST EXPERIMENT: HEALTHY CONTROLS PLASMA SAMPLES

	Gender M/F	**Age at sampling (years)**
n: 29	8M / 17F	60.9 (50.8 – 73)

340

341

342

343

344

345 **Table 1. Demographics and clinical characteristics of ALS (A,B,C) and healthy control**
346 **(D) individuals included in the discovery proteomics (A, B) and in the re-test**
347 **immunoassays (C, D).**
348 The ALS functional rating scale revised (ALSFRS-R; 1 to 48, higher level of neurological
349 disability with lower score) was used to define early (ALSFRS-R ≥ 40) and late (ALSFRS-R
350 ≤ 35) time points in the ALS cohort used for the discovery experiment. ALS patients were
351 stratified according to disease progression rate to last visit (PRL: 48 minus the ALSFRS-R
352 score at the last visit, divided per disease duration from onset in months) in slow (PRL<0.5)
353 and fast (PRL>0.7). PBMC samples were extracted from blood taken from 5 ALS patients with
354 a variable rate of disease progression (B). Age at onset and gender for both patients and healthy
355 matched controls are also reported. All individuals belonged to the same ethnic group
356 (Caucasian; except for one patients who was of Asian ethnicity). Duration of the disease from
357 onset of first symptoms (e.g. weakness or speech impairment) to both sampling time and
358 death/last visit is reported. For each sub-group, values are reported as mean (average).

359

360 **Exploratory analysis using the Feature Selection Tool (FeaST)**

361 Differentially regulated plasma protein signatures across the four phenotypic variants were
362 analysed using principal component analysis (PCA), as illustrated in Fig. 1A. The strongest
363 driver of variance in the data matrix was stage of disease (early *vs*. late), which was captured
364 along the first principal component (Fig. 1A: x-axis) and accounted for approximately 36% of
365 total variance. The rate of disease progression was defined by the second principal component
366 (Fig. 1A: y-axis) and accounted for 15% of total variance (Fig. 1 B, C and D).

367

368 **Functional analysis**

369 Proteome Sciences' proprietary tool for functional analysis (FAT) was used to identify
370 significantly enriched pathways and biological processes in the human and mouse proteomics
371 data. A cross-sectional analysis was undertaken at the early (Fig. 2) and late (additional file 2;
372 supplementary Table 1,1) time points individually using fast vs slow progressing ALS patients
373 as terms of comparison. Fast and slow ALS phenotypic variants were also analysed separately
374 in a longitudinal study, comparing early and late time points (additional file 2; supplementary
375 Table 1, (*2-3*)). The same analytical approach was used to process data from pre-symptomatic
376 and symptomatic fast and slow progressing SOD1G93A transgenic animal models (additional
377 file 2, supplementary Table 1(*2-7*): cross-sectional and longitudinal analysis; additional file 2
378 supplementary Table 4: cross-sectional analysis between SOD1G93A transgenic animals and
379 Wild type littermates)

380

381 Pathway enrichment

382 To avoid redundancy, only those pathways with the highest enrichment values were shown
383 when multiple closely related pathways were identified by FAT. The list of selected pathways
384 is presented in descending order of statistical significance (Fig. 2). In the early stage (Fig. 2A),
385 the strongest differential expression between fast and slow progressing ALS patients was
386 related to proteins involved in ER to Golgi anterograde and retrograde transport, programmed
387 cell death, the immune response linked to MHCII antigen presentation and to pathogenic
388 Escherichia Coli infection. Pathways found to be regulated in both late stage and earlier time
389 point plasma samples included cell cycle (mitosis), apoptosis, protein degradation, post-
390 translational modifications and folding, parkin-ubiquitin proteasomal system, organelle
391 maintenance and membrane transport linked pathways (organelle biogenesis and maintenance,

392 phagosome, and translocation of glucose transporter 4 (GLUT4) to the plasma membrane; Fig.
393 2B). Pathways showing significant enrichment only at the later time point included cellular
394 responses to stress, senescence, vesicular transport, RHO GTPases, RNA regulatory and
395 metabolic processes (Fig. 2C).
396
397 When the slow and fast progressing ALS patients were analysed separately and longitudinally
398 (Fig. 3), the most enriched pathways in slow progressors (Fig. 3A) included DNA damage and
399 telomere stress induced senescence, inflammation and metabolism. In fast progressing ALS
400 patients (Fig. 3C), changes in signal transduction and parkin-ubiquitin proteasomal system
401 pathways were among the most enriched, followed by a cluster of five different pathways
402 sharing a role in the immune response, RNA regulation and protein transport. Notably, in
403 common with the cross-sectional study, the longitudinal analysis identified regulation of
404 proteins involved in cell cycle and signalling, Rho GTPase, membrane trafficking, organelle
405 mediated transport and translocation of GLUT4 to the plasma membrane (Fig. 3 B).
406
407 <u>Gene Ontology (GO) biological processes</u>:
408 In the cross-sectional study, cytoskeleton organization was found enriched in both early and
409 late time points while phagocytosis, epidermis development, membrane organization, innate
410 immune response, ageing and cell division were among the most enriched biological processes
411 only in the early time point. In the late time point, regulation of endopeptidase activity was the
412 top enriched term along with fibrinolysis and proteolysis (additional file 2, supplementary Fig.
413 3).
414
415 In the longitudinal study and in the fast progressing ALS patients, proteins involved in
416 cytoskeletal organization, folding and stabilization, cell adhesion, negative regulation of

417 endopeptidase activity, innate immune response and substantia nigra development were within
418 the most significantly enriched biological features (additional file 2, supplementary Fig. 4B).
419 The analysis of the early versus late time points in the slow progressing patients did not show
420 any significantly enriched biological process.
421
422 Regulated protein candidates:
423 The early disease time point was chosen as the source of most informative differentially
424 expressed plasma protein candidates when comparing ALS-Fast *versus* ALS-Slow (Table 2;
425 proteins containing two or more peptides shown in a top-down order of fold-changes).
426 Additional file 2, table 1 shows the most regulated proteins comparing fast *versus* slow ALS
427 patients in late disease (1), early versus late time points in both fast (2) and Slow (3)
428 progressing ALS patients, as well as those identified in the same cross-sectional (4-5) and
429 longitudinal (6-7) experiment in animal models. The most regulated proteins emerging from
430 the comparison of pre-symptomatic and symptomatic SOD1G93A transgenic mice with their
431 related genetic back-ground WT littermates are reported in additional file 2, table 3.
432 *(For reasons of space and length of the table, **Table 3** has been included further down in the*
433 *paper)*
434

435 Plasma proteomic profile in fast vs slow SOD1 G93A mouse models of ALS and 436 comparability with human pathology

437 Functional analysis for enriched pathways and biological processes (GO terms) in the plasma
438 proteome from the ALS animal models was performed in the same way as for human cases
439 (additional file 2. Supplementary Table 2). Enriched features were compared with those seen
440 in the human arm of the study. There was only a partial overlap in enriched pathways between
441 the human and mouse proteome changes comparing data from the different time points in the

442 two species. Chaperonin mediated protein folding and mitotic processes (pre-symptomatic
443 mouse model, early and late human ALS; Fig. 4A); RHO GTPase activators of IQGAPs
444 (symptomatic mouse model, late human ALS) and apoptosis, anchoring of the basal body to
445 the plasma membrane and AURKA Activation by TPX2 (symptomatic mouse model, early
446 human ALS) (Fig. 4C) were among the pathways shared by human and mouse ALS.
447
448 However, four pathways; assembly of the primary cilium, organelle biogenesis and
449 maintenance, regulation of PLK1 Activity at G2/M transition and translocation of GLUT4 to
450 the plasma membrane were found enriched in both animal models and human disease at all
451 stages considered (Fig. 4A/ 4C).
452
453 With regards to biological processes, cytoskeleton organization was the only feature enriched
454 when comparing fast *versus* slow plasma proteomes from animal and human at the early and
455 late time points (Fig. 4B/ 4D). The acute-phase response GO term was consistently enriched in
456 the pre-symptomatic and symptomatic mouse proteome, but only enriched in the late stage of
457 human disease. The dysregulation of proteolysis pathway was observed only at the late stage
458 in both species. Phagocytosis engulfment was shared between the human early and the
459 symptomatic mouse time points (Fig. 4D).
460
461 **Immunodetection studies**
462 Using immunodetection, we have re-tested the plasma expression of protein candidates
463 belonging to the regulated pathways identified by plasma TMT proteomic analysis in
464 SOD1G93A transgenic mice and in ALS patients, including metabolic processes (APOE,
465 APOA1), acute response, inflammation and cell senescence (ITGB3, Galectin-3, TGFB1).
466 These proteins appear also as regulated in the proteomic analysis comparing WT and

467 SOD1G93A transgenic mice in both genetic back-grounds (additional file 2, **Supplementary**
468 **Table 5**). The re-test experiment was performed using plasma samples from WT129Sv, Pre-
469 SOD1129Sv, Sym-SOD1129Sv, WTC57, Pre-SOD1C57 and Sym-SOD1C57 mice (n:36, 6
470 per sub-group) as well as from ALS patients of the discovery cohort (n:12), re-test cohort (n:
471 47) and from healthy controls (n: 29; Table 1).

472

473 *SOD1G93A transgenic mice*: ITGB3 was significantly up-regulated in plasma from pre-
474 symptomatic SOD1G93A transgenic mice of both fast (129S) and slow (C57) genetic
475 backgrounds compared to both WT and symptomatic mice (Figure 5 A2; Pre-SOD1129Sv p=
476 0.003, Pre-SOD157 p: 0.020). Within the same genotypes, ITGB3 expression decreased
477 significantly in symptomatic SOD1G93A transgenic mice compared to pre-symptomatic
478 (Sym-SOD1C57 p: 0.013; Sym-SOD1129S p: 0.039; Figure 5A). Galectin-3 was down-
479 regulated in plasma from pre-symptomatic and symptomatic SOD1G93A transgenic mice with
480 fast genetic background compared to their WT littermates (Pre-SOD1129Sv p: 0.009; Sym-
481 SOD1129Sv p: 0.004; Figure 5A1), but not in the slow progressing genetic background (Figure
482 5A1). TGFB1 plasma expression increased significantly in pre-symptomatic and symptomatic
483 slow SOD1G93A transgenic mice compared to their WT littermates (Figure 5 A2: Pre-SOD157
484 p: 0.013; Sym-SOD1C57 p: 0.001). Conversely, TGFB1 was down-regulated in pre-
485 symptomatic and symptomatic fast SOD1G93A transgenic mice compared to their WT
486 littermates (Pre-SOD1129Sv p= 0.039; Sym-SOD1129S p: 0.039). There was no statistically
487 significant change of APOE and APOA1 plasma expression between WT and SOD1G93A
488 transgenic mice of both genetic backgrounds (data not shown). For all 5 protein candidates,
489 immunodetection supported the same pattern of expression found in proteomics.

490

491 Analysis of RNA expression of Galectin-3, TGFB1 and ITGB3 in a range of cortical cells [28]
492 showed predominant microglia expression for all three proteins (Figure 5; B, B1, B2 -
493 https://web.stanford.edu/group/barres_lab/brain_rnaseq.html).
494
495 *ALS patients*: APOE was up-regulated in plasma from ALS-Fast compared to ALS-Slow and
496 healthy controls (p: 0.035 and p: 0.041 respectively; Figure 5C). Regression analysis showed
497 a correlation between APOE plasma levels and PRL (p= 0.041; Figure 5C1). Kaplan Mayer
498 analysis identified reduced survival in the higher APOE tertile compared to middle and lower
499 tertiles (p: 0.0156; Figure 4A2) while diagnostic performance by ROC analysis showed APOE
500 levels separate ALS-Fast from ALS-Slow (Area: 0.6759; Std. Error: 0.07162; p: 0.0204).
501 APOE analysis in plasma from the discovery cohort (n:12) showed a trend of over-expression
502 in ALS-fast compared to ALS slow which did not reach significance (data not shown; p: 0.069).
503 There was no statistically significant regulation of Galectine-3, TGFb1, ApoA1 and ITGB3
504 plasma levels at group analysis comparing healthy controls to ALS-FAST and ALS-Slow in
505 both discovery and re-test cohorts, although a trend of up-regulation in ALS-Fast compared to
506 ALS-Slow was seen in both cohorts for these protein candidates (data not shown).
507
508 ITGB3 and Galectin-3 WB analysis was performed on plasma samples from the discovery and
509 re-test cohort, including ALS-Fast (n: 12), ALS-Slow (n:12) and healthy controls (n:10). WB
510 showed a trend of up-regulation for both Galectin-3 and ITGB3 in ALS-Fast compared to ALS-
511 slow which was not significant (data not shown). These results are in line but not in complete
512 agreement with the level of differential regulation seen in the proteomic experiment of the early
513 and late time points (ITGB3 adjusted p value: 0.001111; Galectin adjusted p value: 0.002369;
514 Table 2, additional file 2 supplementary Table 1).
515

516 ## DISCUSSION

517 This study has three unique aspects: 1) a novel quantitative proteomics approach which
518 combines tissue and fluid in a single experiment using TMT® labelling and liquid
519 chromatography combined to mass spectrometry, 2) the use of PBMC, peripheral reporters of
520 central neuro-inflammation [29] as source tissue for plasma biomarker identification and 3) the
521 study of two species (human, mouse) with a comparable phenotypic heterogeneity of the
522 disease.

523

524 We have observed that the rate of ALS progression, and above all the disease stage, are linked
525 to substantial changes in the abundance of a wide range of plasma proteins. In ALS patients
526 and animal models, regulated plasma proteins support a range of inflammatory events and
527 metabolic modifications, while senescence-related alterations are mostly seen with the disease
528 progression in the human ALS proteome. Studying similar phenotypic variants in mouse
529 models and patients with ALS, we have identified only a partial overlap in the overall plasma
530 proteomes acquired in time points which may not necessarily be comparable in the natural
531 history of the disease in humans and rodents. Furthermore, the monogenetic driver of disease
532 in an inbred animal model may only partially reflect the pathological processes of adaptation
533 seen in sporadic human disease, explaining this discrepancy. It is nevertheless encouraging that
534 we could dissect common features that could be developed as translational biomarkers to bridge
535 pre-clinical and human studies.

536 The cross-sectional proteomic studies in human and animals were based on a relatively small
537 sample size. The risk of obtaining non-specific biological signals was mitigated by the
538 inclusion of phenotypic variants and disease time points to test the longitudinal profile of the
539 disease, while a re-test experiment in larger cohorts of WT and transgenic animals as well as
540 of ALS patients and healthy controls, helped to confirm the regulation of relevant protein

541 candidates observed using proteomics, particularly in mouse model. Further investigation of
542 the regulated immuno-metabolic and senescence pathways showed how plasma expression of
543 APOE differentiates ALS patients based on rate of disease progression, while the study of other
544 biomarkers like ITGB3, Galectin-3 and TGFB1 confirmed the pattern of regulation across WT
545 and SOD1G93A transgenic animal models seen in the proteomic experiment. The re-test study
546 by immunodetection did not show the same degree of regulation for ITG3, Galectin-3 and
547 TGFB1 shown in ALS-Fast compared to ALS-Slow using deep proteomics. This can be
548 explained by the small sample size of the discovery cohort used in the proteomic experiment
549 and by the concomitant high phenotypic (and genetic) variability of the disease in human. MS
550 and antibody-based detection techniques have also different analytical sensitivity and
551 specificity, which could also depend on the pre-analytical albumin depletion utilized in
552 proteomics but not in ELISA, as albumin's chaperoning and protein-binding activity may affect
553 the abundance of specific proteins [30]. In the more homogeneous animal models of ALS,
554 proteomic and immunodetection provided comparable results.
555

556 **The plasma/PBMC proteome as a reporter of disease progression in human ALS**

557 PCA indicates that differences in the plasma proteome are more significant between early and
558 late stages of disease, independent of speed of progression (Fig. 1). The selection of ALS
559 patients in an "early" disease stage is complicated by unavoidable diagnostic delays and by
560 poor detection of early signs of "phenoconversion" in asymptomatic individuals. Therefore, in
561 our study, participants were enrolled and sampled at or shortly after diagnosis, and re-sampled
562 after an interval of 6 to 24 and of 48 to 56 months for fast and slow progressing ALS patients
563 respectively (fast and slow ALS patients had comparable ALSFRS-R at the late stage). The
564 change of the plasma proteomic profile in this time-frame includes the early activation of the
565 innate immune response (MCH II signalling), initiation of apoptosis and dysfunction of the

566 proteasome systems which only partially overlap with the pre-symptomatic mouse plasma
567 proteome, while later alterations related to metabolism and glucogenesis as well as RHO
568 GTPase activation are in common with the animal model proteomic (Fig. 2). In our study, RHO
569 GTPase activity is closely linked to a marked regulation of the cytoskeletal proteins
570 organization in both species. RHO GTPase binding to plasma membrane-associated actin
571 cytoskeleton is fundamental to maintain cell-cell and/or cell extracellular matrix (ECM)
572 adhesion [31]. The early immune response activation in our plasma proteome endorses
573 previous reports of a systemic inflammatory response in ALS, involving
574 monocyte/macrophages and a decrease of peripheral T-regulatory cells (Treg) particularly in
575 fast progressing ALS patients, but may also relate to auto-immune disorders which are co-
576 morbid or precede ALS as previously reported [5, 17, 32-34]. However, none of the cases in
577 study had such a history and their blood levels of acute phase reactants, including CRP and
578 ferritin, were within normal limits.
579
580 The prominent expression of proteins involved in the translocation of GLUT4 to the plasma
581 membrane observed in all disease stages under investigation in human and mice, suggests an
582 altered glucose uptake from the blood-stream and a dysmetabolic state (Fig. 2). Lactate, a by-
583 product of cell metabolism which has been reported as raised in blood and CSF from ALS
584 patients, is critically involved in glucose utilization for energy production [35-37]. Recently, it
585 has been proposed that the adenosine triphosphate (ATP)-dependent lactate flow between
586 muscle and neurons at the neuromuscular junction (NMJ) may become disrupted in ALS [38].
587 Extracellular lactate has been shown to cause T cell entrapment at sites of inflammation by
588 inhibition of CD4+ and CD8+ T cells motility, inducing chronic inflammation and a switch of
589 CD4+ T helper cells to a Th17 phenotype with the release of pro-inflammatory cytokines [39].
590 Hence lactate may facilitate chronic inflammation, a key feature of neurodegeneration, while

591 causing NMJ disruption and motor neuron death. Lactate dyscrasia and translocation of
592 GLUT4 to plasma membrane have also been reported to interfere with muscle contraction by
593 loss of GTPase activity [40-44]. The altered GLUT4 translocation and lactate discrasia are
594 among those features potentially bridging human to animal pathology, representing a
595 biologically plausible biomarker and treatment target in ALS.

596

597 **Inflammation, cell senescence and microglial biomarkers in ALS across species**

598 When the differential plasma proteomic profiles of pre-symptomatic and symptomatic
599 transgenic animals were compared to early and late ALS cases, we found inter-species
600 commonalities which included, among others, changes in the acute phase and innate immune
601 responses, protein folding and GTPase Rho signaling (Figure 5). Further analysis of
602 differentially regulated features in our study pointed to microglia activation: 1) the early up-
603 regulation of proteins involved in apoptosis, phagocytosis and of the proteasome system
604 reflecting microglia/macrophage activation which leads to removal of cellular debris and
605 protein aggregates by phagocytosis [45] and 2) ITGB3, Galctin-3 and TGFB1 are selective
606 brain microglia markers, according to a large RNA-Seq transcriptome and splicing database
607 of glia, neurons, and vascular cells of the cerebral cortex
608 (https://web.stanford.edu/group/barres_lab/brain_error_3.html; Figure 5, B,B1,B2).

609

610 Integrins, Galectin-3 and TGFB1 have been implicated in different biological processes
611 including angiogenesis, fibrosis and wound healing [46, 47]. These proteins are also central to
612 the development of the acute phase response leading to chronic tissue injury [48], a molecular
613 feature shared by animal and human ALS plasma proteomes. Critically, ITGB3 has been
614 shown to be a key factor in cell senescence and in the interplay between membrane and ECM
615 through a molecular cascade that includes activation of TGFB1 [49]. Our study also show

616 activation of telomere stress induced senescence with disease progression, implicating ITGB3
617 and TGB1 further in replicative senescence, where telomere length becomes fundamental in
618 loss of cellular homeostasis observed with aging [50]. Astrocyte over-expression of
619 TGFB1accelerates disease progression in ALS mice [51]. ALS skeletal muscle and plasma also
620 show enhanced TGFB1signaling, which can lead to muscle fibrosis [52, 53]. The up-regulation
621 of ITGB3 and TGFB1adds to our previous finding of increased levels of pro-inflammatory
622 cytokines like IL-6 in plasma from ALS patients, a concerted response described as
623 senescence-associated secretory phenotype [6, 54-56].
624
625
626 **ALS: choosing the right therapeutic target and timing for intervention**

627 Any novel treatment strategy for ALS will have to be tested in a more personalized approach,
628 using biomarkers and genetics for clinical stratification [57]. In humans, the lack of any mean
629 of accurate prognostication makes ALS clinical heterogeneity the main obstacle to the
630 development of effective treatments [32]. Conversely, in the relatively homogeneous *SOD1*
631 animal models of ALS, phenotypic variations depend only on expression levels of mutant
632 SOD1, gender, genetic background and possibly on breeding conditions, all features that can
633 be manipulated in a controlled experimental setting [58].
634
635 Our study has shown a convergence between species in molecular mechanisms centered around
636 regulation of the immune response and of cell metabolism. These shared regulated pathways
637 support the potential for early immune-modulatory strategies, including the use of anti-
638 inflammatory compounds, stem-cell based immune-effective treatment or protein kinase
639 inhibitors, used to stem microglia-mediated neuroinflammation [21, 59, 60]. While fighting
640 this innate immune response as early as possible may be plausible, it is worth considering that

macrophages at this stage and potentially throughout the disease course clear debris from cells undergoing degeneration. This "beneficial" inflammatory response may later shift towards a chronic and harmful process [6, 45, 61-65]. Therefore, timing of immunomodulation in ALS is crucial and interventions must aim at the window of therapeutic opportunity to arrest any development to chronic inflammation, which is an integral part of cell senescence and of the SASP response. Inducers of heat shock response have been shown to efficiently inhibit and reduce chronic inflammation in obesity and the same therapeutic paradigm may be relevant in neuroinflammation [66].

Our findings support also treatment strategies which target the enzymatic chain of glucose metabolism leading to the production of lactate, based on the combination of drugs that inhibit lactate accumulation at the NMJ and its effect in reducing T-cell migratory capabilities, enhancing respiratory chain function, and/or promoting re-innervation [38]. Interestingly, nutritional supplements acting at the interface between inflammation and metabolism have been shown to dampen the inflammatory environment. For example, omega-3 essential fatty acids decrease the levels of IL-1, IL-6, TNFα and CRP [67] and improve cognitive function in aged mice [68].

CONCLUSIONS

This study provides one of the most in-depth qualitative and quantitative proteomics studies performed in ALS, using the plasma/PBMC interface to investigate crucial aspects of phenotypic heterogeneity of this condition and across species. Researchers working on ALS and on other neurodegenerative disorders will be able to draw on the data we have generated to steer the development of novel biomarkers and therapeutic strategies in ALS.

667 **LIST OF ABBREVIATIONS**

ALS (amyotrophic lateral sclerosis)

ALSFRS-R (amyotrophic lateral sclerosis Functional Rating Scale-Revised)

CRP (C-reactive protein)

ECM (extracellular matrix)

EDTA (Ethylenediaminetetraacetic acid)

ER (Endoplasmatic Reticulum)

FBS (Fetal bovine serum)

FTD (frontotemporal dementia)

HRP (horseradish peroxidase)

IL (interleukin)

ITGB3 (integrin Beta 3)

LC-MS/MS (liquid chromatography tandem mass spectrometry)

LIMMA (linear models for microarray data)

logFC (Log2 fold changes)

MHC (major histocompatibility complex)

NMJ (neuromuscular junction)

PBMC (peripheral Blood Mononuclear Cells)

PBS (phosphate buffered saline)

PCA (principal component analysis)

PRL (disease progression to last visit)

PSM (peptide spectrum matches),

RT (room temperature)

SASP (senescence-associated secretory phenotype)

SCX (Strong Cation exchange)

SOD1 (superoxide dismutase 1)

TBST (tris buffered saline- tween)

TCEP (tris (2-carboxyethyl) phosphine 10)

TDP-43 (TAR DNA-binding protein 43)

TEAB (triethylammonium bicarbonate)

TGF-β1 (transforming growth factor beta 1)

TMT (tandem mass tag)

TNFα (tumor necrosis factor alpha)

668 **DECLARATIONS**

669 **Ethics approval and consent to participate**

670 Ethical approval was obtained from the East London and the City Research Ethics Committee
671 1 (09/H0703/27). All participants provided written consent to the study (or gave verbal
672 permission for a carer to sign on their behalf).

673 Procedures involving animals and their care were conducted in conformity with institutional
674 guidelines that comply with national (Legislative Degree 26.03.2014) and international (EEC
675 Council Directive 2010/63, August, 2013) laws and policies. Animals studies were approved
676 by the Mario Negri Institute Animal Care and Use Committee and by the Italian Ministerial
677 decree no. 84-2013.

678 **Consent for publication**

679 Not applicable

680 **Availability of data and material**

681 All data generated or analysed during this study are included in this published article and its
682 supplementary information files as additional files.

683 Additional file 1 (pdf). Detailed protocols for Sample fractionation, LC-MS/MS analysis and
684 peptide identification and quantification: methods are explained in more detail in this additional
685 file.

686 Additional file 2 (pdf.) Supplementary figures and tables: foursupplementary figures and 2
687 supplementary tables are presented in this file. Supplementary figure 1 represents and scheme
688 of the workflow followed to perform this study. Supplementary figure 2 shows the PCA before
689 batch effect correction, Supplementary figure 3, illustrates the uncut and un edited western blot
690 results together with the Ponceau staining for the membranes, supplementary figure 4 shows
691 enriched biological processes for the cross-sectional and longitudinal study. Additional table 1
692 shows the top regulated proteins in plasma from 1) fast versus slow progressing ALS patients
693 at the late stage disease, early versus late time points for slow and fast progressing ALS patients
694 and mouse model: cross sectional and longitudinal studies. Supplementary table 2 where the
695 functional analysis of the animal model proteomic data are presented.

696 Additional file 3 (csv.) contains all the raw data generated in the human analysis

697 Additional file 4 (csv.) contains all the raw data generated in the animal model analysis.

698

699 **Competing interests**

700 The authors declare that they have no competing interests.

701 **Funding**

702 Motor Neurone Disease Association (Malaspina/Apr13/817-791). Wellcome Trust support to
703 a parallel study (Pathfinder Award, grant number 103208).

704 **Author contribution**

705 IZ is the lead author who has worked on the design, conduction of experiments and analysis of
706 the data and contributed to manuscript writing. VL has performed all the Mesoscale assays and
707 validation processes. MB and VM were responsible for data processing, bioinformatics method
708 development and execution. MB has also developed the functional analysis tool employed in
709 this study. GN and CB have been in charge of breeding and sampling of the animal model used
710 in this study. RA, VL, OY and CHL have worked on the human samples collection, processing
711 and storage, while contributing to sample selection, RA has also performed some of the Integrin
712 beta 3 western blot experiments. EL, MW, PY contributed to the experimental design. AM and
713 IP have conceived the study design and led on all the aspects including bio banking,
714 experimental procedures, data interpretation and manuscript writing. AM was awarded he
715 grant that has made this study possible. LG has contributed to the project design and
716 supervision. AM was the group leader of this project leading on patient recruitment, guidance,
717 paper writing and study design.

718

719 **Acknowledgments**

720 We acknowledge the patients and their families for kindly agreeing to collaborate in this
721 project, the authors would also like to thank Gitte Boehm for her assistance on sample
722 preparation for the animal model experiments, other colleagues in Proteome Sciences in
723 Frankfurt and Proteome Sciences London, in particular Eva Sedlak and Richard Churchus for
724 the mass spectrometry data acquisition.

725

726 **FIGURESLEGENDS AND TABLE**

727

728 **Figure 1. Distribution of differentially regulated features and ALS patient phenotypic**
729 **variants:** (A) Principal component analysis (PCA) using scores plots before feature selection
730 (colour codes: fast-early: yellow; fast-late: green; slow-early: red; slow-late: brown). The
731 disease stage dimension is the main contributor to the separation in the first component
732 (35.86%) and the rate of disease progression is the main contributor to the separation on the
733 second component (15%). (B) PCA loadings plot generated with data derived from regulated
734 features shows a more significant separation in the first compared to second component (40.6%
735 and 17.5% respectively). (C) Volcano plot showing significantly regulated features comparing
736 fast and slow progressing ALS patients in the early time point (cross-sectional study). (D)
737 Volcano plot showing significantly regulated features comparing early and late time points for
738 the slow progressing ALS patients (longitudinal study). Volcano plots agree with PCA showing
739 a more significant difference between early and late time points when compared to fast versus
740 slow disease progression.

741 **Figure 2. Functional analysis of the proteomic data obtained comparing data from fast**
742 **versus slow progressing ALS patients.**

743 The cross-sectional analysis was based on the list of regulated proteins (FC 1.3, p value <
744 0.05). Pathways with a p value < 0.05 were considered significantly enriched and–plotted
745 with a -log 10 transformed p value. Functional analysis was performed for Reactome
746 pathways, if not otherwise specified. Only the pathways with the highest enrichment were
747 reported among the selected redundant pathways (mostly cell cycle and mitosis (early) and
748 RHO GTPase (late)). Significantly enriched pathways in the early stage (A), late stage (C)
749 and in both time points (B).

750

751 **Figure 3. Functional analysis of the proteomic data obtained comparing early versus late**
752 **disease stage.**

753 The longitudinal analysis was undertaken using the list of total regulated proteins (FC 1.3, p
754 value < 0.05) in slow and fast progressing ALS individuals independently. Pathways with a p
755 value < 0.05 were considered significantly enriched and plotted with a - log 10 transformed p
756 value in descending order of statistical significance. Functional analysis was performed for
757 Reactome pathways, if not otherwise specified. Only pathways with the highest enrichment
758 were reported among redundant pathways. Significantly enriched pathways in slow
759 progressing patients (A), in fast progressing patients (C) and shared by slow and fast
760 progressing patients (B).

761

762 **Figure 5. Re-test of protein candidates using immunoassays**
763 ELISA and Meso Scale Discovery (MSD) analysis of selected protein candidates in plasma
764 samples. **A.** APOE is up-regulated in plasma samples from ALS-Fast compared to ALS-Slow;
765 **A1**: positive correlation between APOE plasma levels and PRL in ALS patients; **A2**: reduced
766 survival for ALS patient with higher APOE levels (above 70776 pg/ml). **B.** Galectin-3 is
767 significantly downregulated in pre-symptomatic (Pre-SOD1129Sv) and fast in progressing
768 SOD1G93A transgenic mice (Sym-SOD1129Sv) compared to 129Sv WT animals (WT129Sv).
769 **B1.** TGFB1 is significantly downregulated in plasma from Pre-SOD1C57 and from Sym-
770 SOD1C57 compared to WTC57, while it upregulated up-regulated in Pre-SOD1129Sv and
771 Sym-SOD1129Sv compared to WT129Sv. **B2**. ITGB3 is up-regulated in plasma from pre-
772 symptomatic transgenic SOD1G93 animal models (Pre-SOD1129Sv, Pre-SOD1C57)
773 compared to related WT animals, while ITGB3 plasma expression in the respective
774 symptomatic animals are significantly reduces to WT levels. In each figure, reported upper p-
775 values relate to Kruskall-Wallis while lower p-values to Dunn's multiple comparisons tests.

776 **C.** data mining using a RNA-Seq transcriptome and splicing database of glia, neurons, and
777 vascular cells of the cerebral cortex. This interactive splicing browser shows predominant
778 microglia expression of Galectin-3 (C), TGFB1(C1) and ITGB3 (C2)
779 (https://web.stanford.edu/group/barres_lab/brain_rnaseq.html) in a range of cortical cells[28].
780 PRL: progression rate to last visit.
781 WT: wild type.
782 OPC: oligodendrocyte precursor cells.
783 FPKM: fragments per kilobase of transcript sequence per million mapped fragments.
784
785
786
787 **Figure 6. Human-animal model comparison of enriched pathways (A and C) and**
788 **biological processes (B and D) derived from regulated proteins in each specie**. (A) Shows
789 the pathways and (B) the biological processes that were found enriched in both the mouse
790 model pre-symptomatic stage and in the human ALS proteome at an early and a late disease
791 stage respectively. (C) Shows the pathways and (D) the biological processes found enriched in
792 both the mouse model symptomatic stage and the human ALS proteome at an early and late
793 disease stage respectively. Pathways and biological processes, including translocation of
794 GLUT4 to the plasma membrane or acute-phase response, that were found regulated in both
795 mouse model and human plasma proteome at all time points are indicated with an asterisk (*).
796

797

798

799

800

801

	Protein ID	Protein Descriptions	Gene Name	Peptide #	Early _Fast/Early Slow Log Fold Change	adjusted p-value
Up regulated in FAST. Early stage.	P05106	Integrin beta-3	ITGB3	2	2.224407	0.001111
	O95810	Serum deprivation-response protein	SDPR	3	2.102	0.001403
	H7BYX 6	Isoform of P13591, Neural cell adhesion molecule 1	NCAM1	2	2.027403	0.000418
	P04003	C4b-binding protein alpha chain	C4BPA	7	2.013732	8.04E-05
	P07437	Tubulin beta chain	TUBB	2	1.908567	0.00790
	P63173	60S ribosomal protein L38	RPL38	2	1.727873	0.00652
	Q14697	Neutral alpha-glucosidase AB	GANAB	2	1.638215	0.00134
	P02649	Apolipoprotein E	APOE	9	1.513701	8.53E-05
	P36957	Dihydrolipoyllysine-residue succinyltransferase component of 2-oxoglutarate	DLST	2	1.487187	0.00960

		dehydrogenase complex, mitochondrial				
	A0A0A0MR02	Isoform of P45880, Voltage-dependent anion-selective channel protein 2	VDAC2	4	1.4397	0.00229
	P05090	Apolipoprotein D	APOD	6	1.293627	0.00240
	P80723	Brain acid soluble protein 1	BASP1	4	1.220442	0.00111
	P15169	Carboxypeptidase N catalytic chain	CPN1	3	1.17725	0.00616
	Q06033-2	Isoform of Q06033, Isoform 2 of Inter-alpha-trypsin inhibitor heavy chain H3	ITIH3	4	1.176924	0.00172
	P48740-2	Isoform of P48740, Isoform 2 of Mannan-binding lectin serine protease 1	MASP1	2	1.126878	0.00134
	P35527	Keratin, type I cytoskeletal 9	KRT9	6	1.061453	0.00827
	Q15582	Transforming growth factor-beta-induced protein ig-h3	TGFBI	3	1.026849	0.00652
	P07355	Annexin A2	ANXA2	6	1.021165	0.00788
Down regulated in FAST Early stage.	P69905	Hemoglobin subunit alpha	HBA1	6	-1.12687	0.00682
	E7ETH0	Isoform of P05156, Complement factor I	CFI	3	-1.14553	0.00190
	O75636-2	Isoform of O75636, Isoform 2 of Ficolin-3	FCN3	4	-1.16238	0.00616
	Q96IY4	Carboxypeptidase B2	CPB2	2	-1.23801	0.00134

	P05452	Tetranectin	CLEC3B	2	-1.32297	0.00173
	P30050	60S ribosomal protein L12	RPL12	2	-1.50426	0.00172
	P20700	Lamin-B1	LMNB1	2	-1.86089	0.00728
	P00505	Aspartate aminotransferase, mitochondrial	GOT2	2	-2.47293	0.00172
	P02042	Hemoglobin subunit delta	HBD	3	-2.49876	0.00040
	Q5T123	Isoform of Q9H299, SH3 domain-binding glutamic acid-rich-like protein 3	SH3BGR L3	2	-2.75577	0.0011

802

803 **Table 2. Regulated proteins in fast compared to slow progressing ALS patients in the early**
804 **disease stage**. Only proteins identified with at least two unique peptides are shown. Up-
805 regulated proteins are shown in the upper part of the table (grey), with Integrin beta-3 showing
806 the highest fold change. Down-regulated proteins are shown in the bottom part of the table
807 (light blue), with Isoform of Q9H299, SH3 domain-binding glutamic acid-rich-like protein 3,
808 showing the highest fold change of all down-regulated proteins.

809

810

811 ## REFERENCES

812

813

814 1. Chio A, Logroscino G, Hardiman O, Swingler R, Mitchell D, Beghi E, Traynor BG:
815 **Prognostic factors in ALS: A critical review.** *Amyotrophic lateral sclerosis :*
816 *official publication of the World Federation of Neurology Research Group on Motor*
817 *Neuron Diseases* 2009, **10:**310-323.

818 2. Baumer D, Talbot K, Turner MR: **Advances in motor neurone disease.** *Journal of*
819 *the Royal Society of Medicine* 2014, **107:**14-21.
820 3. Ittner LM, Halliday GM, Kril JJ, Gotz J, Hodges JR, Kiernan MC: **FTD and ALS--**
821 **translating mouse studies into clinical trials.** *Nature reviews Neurology* 2015,
822 **11:**360-366.
823 4. Petrov D, Mansfield C, Moussy A, Hermine O: **ALS Clinical Trials Review: 20**
824 **Years of Failure. Are We Any Closer to Registering a New Treatment?** *Frontiers*
825 *in aging neuroscience* 2017, **9:**68.
826 5. Henkel JS, Beers DR, Wen S, Rivera AL, Toennis KM, Appel JE, Zhao W, Moore
827 DH, Powell SZ, Appel SH: **Regulatory T-lymphocytes mediate amyotrophic**
828 **lateral sclerosis progression and survival.** *EMBO molecular medicine* 2013, **5:**64-
829 79.
830 6. Lu CH, Allen K, Oei F, Leoni E, Kuhle J, Tree T, Fratta P, Sharma N, Sidle K,
831 Howard R, et al: **Systemic inflammatory response and neuromuscular**
832 **involvement in amyotrophic lateral sclerosis.** *Neurology(R) neuroimmunology &*
833 *neuroinflammation* 2016, **3:**e244.
834 7. Nardo G, Trolese MC, Bendotti C: **Major Histocompatibility Complex I**
835 **Expression by Motor Neurons and Its Implication in Amyotrophic Lateral**
836 **Sclerosis.** *Frontiers in neurology* 2016, **7:**89.
837 8. Marino M, Papa S, Crippa V, Nardo G, Peviani M, Cheroni C, Trolese MC,
838 Lauranzano E, Bonetto V, Poletti A, et al: **Differences in protein quality control**
839 **correlate with phenotype variability in 2 mouse models of familial amyotrophic**
840 **lateral sclerosis.** *Neurobiology of aging* 2015, **36:**492-504.
841 9. Schmitt F, Hussain G, Dupuis L, Loeffler JP, Henriques A: **A plural role for lipids**
842 **in motor neuron diseases: energy, signaling and structure.** *Frontiers in cellular*
843 *neuroscience* 2014, **8:**25.
844 10. Liu G, Fiala M, Mizwicki MT, Sayre J, Magpantay L, Siani A, Mahanian M,
845 Chattopadhyay M, La Cava A, Wiedau-Pazos M: **Neuronal phagocytosis by**
846 **inflammatory macrophages in ALS spinal cord: inhibition of inflammation by**
847 **resolvin D1.** *American journal of neurodegenerative disease* 2012, **1:**60-74.
848 11. Taylor JP, Brown RH, Jr., Cleveland DW: **Decoding ALS: from genes to**
849 **mechanism.** *Nature* 2016, **539:**197-206.
850 12. Howlett DR: **Protein Misfolding in Disease: Cause or Response?** *Current*
851 *Medicinal Chemistry - Immunology, Endocrine & Metabolic Agents* 2003, **3:**371-383.
852 13. Edbauer D, Haass C: **An amyloid-like cascade hypothesis for C9orf72 ALS/FTD.**
853 *Current opinion in neurobiology* 2016, **36:**99-106.
854 14. Buchberger A, Bukau B, Sommer T: **Protein quality control in the cytosol and the**
855 **endoplasmic reticulum: brothers in arms.** *Molecular cell* 2010, **40:**238-252.
856 15. Yin F, Sancheti H, Patil I, Cadenas E: **Energy metabolism and inflammation in**
857 **brain aging and Alzheimer's disease.** *Free radical biology & medicine* 2016,
858 **100:**108-122.
859 16. Ngo ST, Steyn FJ: **The interplay between metabolic homeostasis and**
860 **neurodegeneration: insights into the neurometabolic nature of amyotrophic**
861 **lateral sclerosis.** *Cell regeneration (London, England)* 2015, **4:**5.
862 17. Malaspina A, Puentes F, Amor S: **Disease origin and progression in amyotrophic**
863 **lateral sclerosis: an immunology perspective.** *International immunology* 2015,
864 **27:**117-129.
865 18. Rossi S, Zanier ER, Mauri I, Columbo A, Stocchetti N: **Brain temperature, body**
866 **core temperature, and intracranial pressure in acute cerebral damage.** *J Neurol*
867 *Neurosurg Psychiatry* 2001, **71:**448-454.

868 19. van der Worp HB, Howells DW, Sena ES, Porritt MJ, Rewell S, O'Collins V,
869 Macleod MR: **Can animal models of disease reliably inform human studies?** *PLoS*
870 *medicine* 2010, **7:**e1000245.
871 20. Moujalled D, White AR: **Advances in the Development of Disease-Modifying**
872 **Treatments for Amyotrophic Lateral Sclerosis.** *CNS drugs* 2016, **30:**227-243.
873 21. Gordon PH, Moore DH, Miller RG, Florence JM, Verheijde JL, Doorish C, Hilton JF,
874 Spitalny GM, MacArthur RB, Mitsumoto H, et al: **Efficacy of minocycline in**
875 **patients with amyotrophic lateral sclerosis: a phase III randomised trial.** *Lancet*
876 *Neurol* 2007, **6:**1045-1053.
877 22. Nardo G, Pozzi S, Pignataro M, Lauranzano E, Spano G, Garbelli S, Mantovani S,
878 Marinou K, Papetti L, Monteforte M, et al: **Amyotrophic lateral sclerosis**
879 **multiprotein biomarkers in peripheral blood mononuclear cells.** *PloS one* 2011,
880 **6:**e25545.
881 23. Filareti M, Luotti S, Pasetto L, Pignataro M, Paolella K, Messina P, Pupillo E, Filosto
882 M, Lunetta C, Mandrioli J, et al: **Decreased Levels of Foldase and Chaperone**
883 **Proteins Are Associated with an Early-Onset Amyotrophic Lateral Sclerosis.**
884 *Frontiers in molecular neuroscience* 2017, **10:**99.
885 24. Russell CL, Heslegrave A, Mitra V, Zetterberg H, Pocock JM, Ward MA, Pike I:
886 **Combined tissue and fluid proteomics with Tandem Mass Tags to identify low-**
887 **abundance protein biomarkers of disease in peripheral body fluid: An**
888 **Alzheimer's Disease case study.** *Rapid communications in mass spectrometry : RCM*
889 2017, **31:**153-159.
890 25. Nardo G, Trolese MC, Tortarolo M, Vallarola A, Freschi M, Pasetto L, Bonetto V,
891 Bendotti C: **New Insights on the Mechanisms of Disease Course Variability in**
892 **ALS from Mutant SOD1 Mouse Models.** *Brain pathology (Zurich, Switzerland)*
893 2016, **26:**237-247.
894 26. Pizzasegola C, Caron I, Daleno C, Ronchi A, Minoia C, Carri MT, Bendotti C:
895 **Treatment with lithium carbonate does not improve disease progression in two**
896 **different strains of SOD1 mutant mice.** *Amyotrophic lateral sclerosis : official*
897 *publication of the World Federation of Neurology Research Group on Motor Neuron*
898 *Diseases* 2009, **10:**221-228.
899 27. Brooks BR: **Functional scales: summary.** *Amyotrophic lateral sclerosis and other*
900 *motor neuron disorders : official publication of the World Federation of Neurology,*
901 *Research Group on Motor Neuron Diseases* 2002, **3 Suppl 1:**S13-18.
902 28. Zhang Y, Chen K, Sloan SA, Bennett ML, Scholze AR, O'Keeffe S, Phatnani HP,
903 Guarnieri P, Caneda C, Ruderisch N, et al: **An RNA-sequencing transcriptome and**
904 **splicing database of glia, neurons, and vascular cells of the cerebral cortex.** *J*
905 *Neurosci* 2014, **34:**11929-11947.
906 29. Koncarevic S, Lossner C, Kuhn K, Prinz T, Pike I, Zucht HD: **In-depth profiling of**
907 **the peripheral blood mononuclear cells proteome for clinical blood proteomics.**
908 *International journal of proteomics* 2014, **2014:**129259.
909 30. Finn TE, Nunez AC, Sunde M, Easterbrook-Smith SB: **Serum albumin prevents**
910 **protein aggregation and amyloid formation and retains chaperone-like activity**
911 **in the presence of physiological ligands.** *J Biol Chem* 2012, **287:**21530-21540.
912 31. Govek EE, Newey SE, Van Aelst L: **The role of the Rho GTPases in neuronal**
913 **development.** *Genes Dev* 2005, **19:**1-49.
914 32. Turner MR, Bowser R, Bruijn L, Dupuis L, Ludolph A, McGrath M, Manfredi G,
915 Maragakis N, Miller RG, Pullman SL, et al: **Mechanisms, models and biomarkers**
916 **in amyotrophic lateral sclerosis.** *Amyotrophic lateral sclerosis & frontotemporal*
917 *degeneration* 2013, **14 Suppl 1:**19-32.

918 33. Rentzos M, Rombos A, Nikolaou C, Zoga M, Zouvelou V, Dimitrakopoulos A,
919 Alexakis T, Tsoutsou A, Samakovli A, Michalopoulou M, Evdokimidis J:
920 **Interleukin-17 and interleukin-23 are elevated in serum and cerebrospinal fluid**
921 **of patients with ALS: a reflection of Th17 cells activation?** *Acta neurologica*
922 *Scandinavica* 2010, **122:**425-429.
923 34. Bowerman M, Vincent T, Scamps F, Perrin FE, Camu W, Raoul C: **Neuroimmunity**
924 **dynamics and the development of therapeutic strategies for amyotrophic lateral**
925 **sclerosis.** *Frontiers in cellular neuroscience* 2013, **7:**214.
926 35. Zaid H, Antonescu CN, Randhawa VK, Klip A: **Insulin action on glucose**
927 **transporters through molecular switches, tracks and tethers.** *The Biochemical*
928 *journal* 2008, **413:**201-215.
929 36. Medina RA, Southworth R, Fuller W, Garlick PB: **Lactate-induced translocation of**
930 **GLUT1 and GLUT4 is not mediated by the phosphatidyl-inositol-3-kinase**
931 **pathway in the rat heart.** *Basic research in cardiology* 2002, **97:**168-176.
932 37. Lee Y, Morrison BM, Li Y, Lengacher S, Farah MH, Hoffman PN, Liu Y, Tsingalia
933 A, Jin L, Zhang P-W, et al: **Oligodendroglia metabolically support axons and**
934 **contribute to neurodegeneration.** *Nature* 2012, **487:**443-448.
935 38. Vadakkadath Meethal S, Atwood CS: **Lactate dyscrasia: a novel explanation for**
936 **amyotrophic lateral sclerosis.** *Neurobiology of aging* 2012, **33:**569-581.
937 39. Haas R, Cucchi D, Smith J, Pucino V, Macdougall CE, Mauro C: **Intermediates of**
938 **Metabolism: From Bystanders to Signalling Molecules.** *Trends in biochemical*
939 *sciences* 2016, **41:**460-471.
940 40. Leney SE, Tavare JM: **The molecular basis of insulin-stimulated glucose uptake:**
941 **signalling, trafficking and potential drug targets.** *The Journal of endocrinology*
942 2009, **203:**1-18.
943 41. Bogan JS, Kandror KV: **Biogenesis and regulation of insulin-responsive vesicles**
944 **containing GLUT4.** *Current opinion in cell biology* 2010, **22:**506-512.
945 42. Foley K, Boguslavsky S, Klip A: **Endocytosis, recycling, and regulated exocytosis**
946 **of glucose transporter 4.** *Biochemistry* 2011, **50:**3048-3061.
947 43. Hoffman NJ, Elmendorf JS: **Signaling, cytoskeletal and membrane mechanisms**
948 **regulating GLUT4 exocytosis.** *Trends in endocrinology and metabolism: TEM* 2011,
949 **22:**110-116.
950 44. Kandror KV, Pilch PF: **The sugar is sIRVed: sorting Glut4 and its fellow**
951 **travelers.** *Traffic (Copenhagen, Denmark)* 2011, **12:**665-671.
952 45. Heneka MT, Golenbock DT, Latz E: **Innate immunity in Alzheimer's disease.**
953 *Nature immunology* 2015, **16:**229-236.
954 46. Margadant C, Sonnenberg A: **Integrin-TGF-beta crosstalk in fibrosis, cancer and**
955 **wound healing.** *EMBO reports* 2010, **11:**97-105.
956 47. Desgrosellier JS, Cheresh DA: **Integrins in cancer: biological implications and**
957 **therapeutic opportunities.** *Nature reviews Cancer* 2010, **10:**9-22.
958 48. Gawlik KI, Holmberg J, Svensson M, Einerborg M, Oliveira BM, Deierborg T,
959 Durbeej M: **Potent pro-inflammatory and pro-fibrotic molecules, osteopontin and**
960 **galectin-3, are not major disease modulators of laminin alpha2 chain-deficient**
961 **muscular dystrophy.** *Scientific reports* 2017, **7:**44059.
962 49. Rapisarda V, Borghesan M, Miguela V, Encheva V, Snijders AP, Lujambio A,
963 O'Loghlen A: **Integrin Beta 3 Regulates Cellular Senescence by Activating the**
964 **TGF-beta Pathway.** *Cell reports* 2017, **18:**2480-2493.
965 50. Victorelli S, Passos JF: **Telomeres and Cell Senescence - Size Matters Not.**
966 *EBioMedicine* 2017, **21:**14-20.

967 51. Endo F, Komine O, Fujimori-Tonou N, Katsuno M, Jin S, Watanabe S, Sobue G,
968 Dezawa M, Wyss-Coray T, Yamanaka K: **Astrocyte-derived TGF-beta1 accelerates**
969 **disease progression in ALS mice by interfering with the neuroprotective**
970 **functions of microglia and T cells.** *Cell reports* 2015, **11:**592-604.
971 52. Gonzalez D, Contreras O, Rebolledo DL, Espinoza JP, van Zundert B, Brandan E:
972 **ALS skeletal muscle shows enhanced TGF-beta signaling, fibrosis and induction**
973 **of fibro/adipogenic progenitor markers.** *PloS one* 2017, **12:**e0177649.
974 53. Houi K, Kobayashi T, Kato S, Mochio S, Inoue K: **Increased plasma TGF-beta1 in**
975 **patients with amyotrophic lateral sclerosis.** *Acta neurologica Scandinavica* 2002,
976 **106:**299-301.
977 54. Freund A, Orjalo AV, Desprez PY, Campisi J: **Inflammatory networks during**
978 **cellular senescence: causes and consequences.** *Trends in molecular medicine* 2010,
979 **16:**238-246.
980 55. Chinta SJ, Woods G, Rane A, Demaria M, Campisi J, Andersen JK: **Cellular**
981 **senescence and the aging brain.** *Experimental gerontology* 2015, **68:**3-7.
982 56. Ovadya Y, Krizhanovsky V: **Senescent cells: SASPected drivers of age-related**
983 **pathologies.** *Biogerontology* 2014, **15:**627-642.
984 57. Picher-Martel V, Valdmanis PN, Gould PV, Julien JP, Dupre N: **From animal**
985 **models to human disease: a genetic approach for personalized medicine in ALS.**
986 *Acta neuropathologica communications* 2016, **4:**70.
987 58. Pfohl SR, Halicek MT, Mitchell CS: **Characterization of the Contribution of**
988 **Genetic Background and Gender to Disease Progression in the SOD1 G93A**
989 **Mouse Model of Amyotrophic Lateral Sclerosis: A Meta-Analysis.** *Journal of*
990 *neuromuscular diseases* 2015, **2:**137-150.
991 59. Karussis D, Karageorgiou C, Vaknin-Dembinsky A, Gowda-Kurkalli B, Gomori JM,
992 Kassis I, Bulte JW, Petrou P, Ben-Hur T, Abramsky O, Slavin S: **Safety and**
993 **immunological effects of mesenchymal stem cell transplantation in patients with**
994 **multiple sclerosis and amyotrophic lateral sclerosis.** *Archives of neurology* 2010,
995 **67:**1187-1194.
996 60. Lee SH, Suk K: **Emerging roles of protein kinases in microglia-mediated**
997 **neuroinflammation.** *Biochemical pharmacology* 2017.
998 61. Bronzuoli MR, Iacomino A, Steardo L, Scuderi C: **Targeting neuroinflammation in**
999 **Alzheimer's disease.** *Journal of inflammation research* 2016, **9:**199-208.
1000 62. Krauthausen M, Saxe S, Zimmermann J, Emrich M, Heneka MT, Muller M: **CXCR3**
1001 **modulates glial accumulation and activation in cuprizone-induced demyelination**
1002 **of the central nervous system.** *Journal of neuroinflammation* 2014, **11:**109.
1003 63. Pal R, Tiwari PC, Nath R, Pant KK: **Role of neuroinflammation and latent**
1004 **transcription factors in pathogenesis of Parkinson's disease.** *Neurological*
1005 *research* 2016, **38:**1111-1122.
1006 64. Dibaj P, Steffens H, Zschuntzsch J, Nadrigny F, Schomburg ED, Kirchhoff F, Neusch
1007 C: **In Vivo imaging reveals distinct inflammatory activity of CNS microglia**
1008 **versus PNS macrophages in a mouse model for ALS.** *PloS one* 2011, **6:**e17910.
1009 65. Hornik TC, Vilalta A, Brown GC: **Activated microglia cause reversible apoptosis**
1010 **of pheochromocytoma cells, inducing their cell death by phagocytosis.** *Journal of*
1011 *cell science* 2016, **129:**65-79.
1012 66. Newsholme P, de Bittencourt PI, Jr.: **The fat cell senescence hypothesis: a**
1013 **mechanism responsible for abrogating the resolution of inflammation in chronic**
1014 **disease.** *Current opinion in clinical nutrition and metabolic care* 2014, **17:**295-305.
1015 67. Simopoulos AP: **Omega-3 fatty acids in inflammation and autoimmune diseases.**
1016 *Journal of the American College of Nutrition* 2002, **21:**495-505.

1017 68. Cutuli D, De Bartolo P, Caporali P, Laricchiuta D, Foti F, Ronci M, Rossi C, Neri C,
1018 Spalletta G, Caltagirone C, et al: **n-3 polyunsaturated fatty acids supplementation**
1019 **enhances hippocampal functionality in aged mice.** *Frontiers in aging neuroscience*
1020 2014, **6:**220.
1021

1022

1023 Figure 1

1024

1025

1026 Figure 2

1027

1028 Figure 3

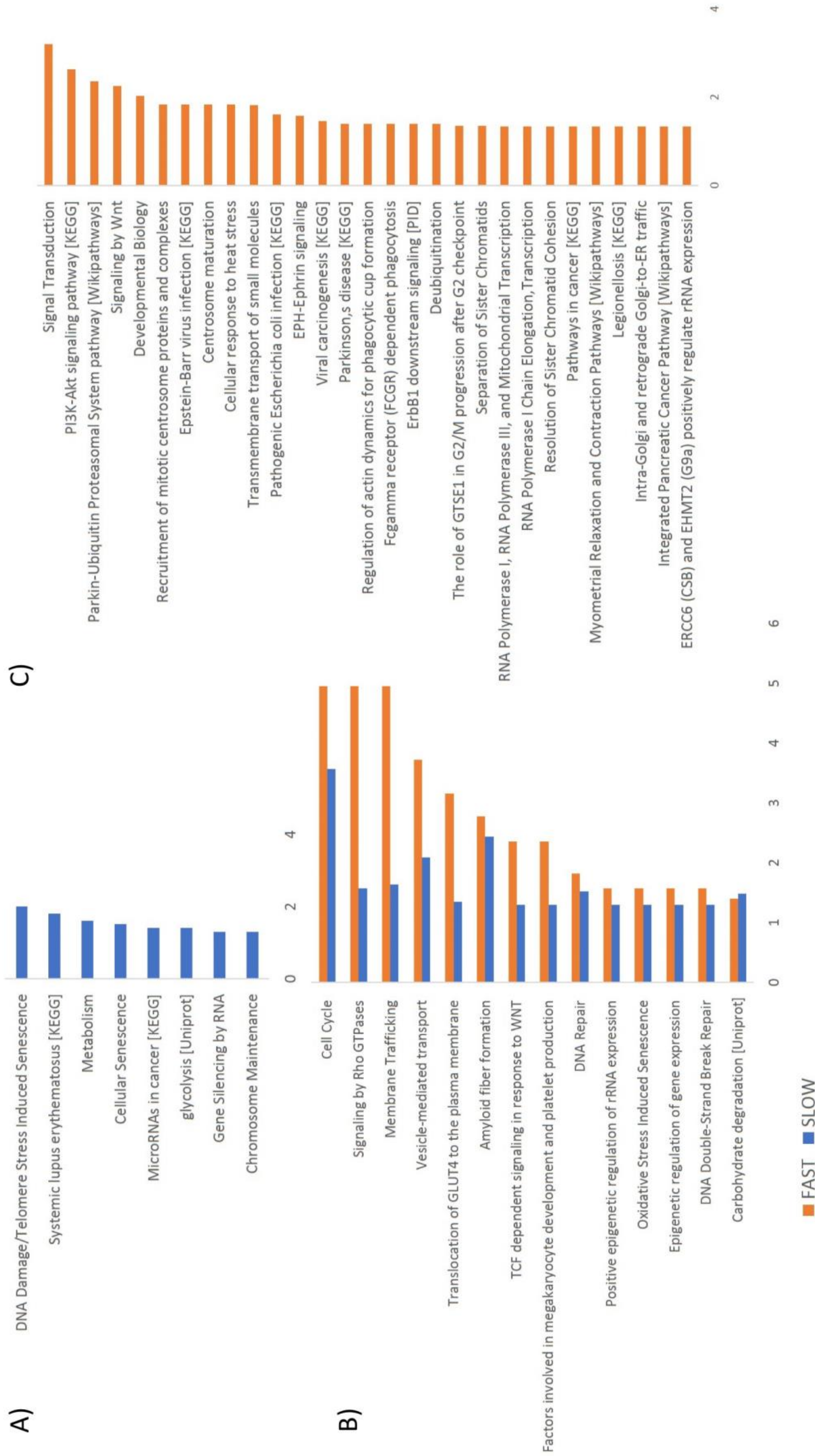

1029

1030 Figure 4

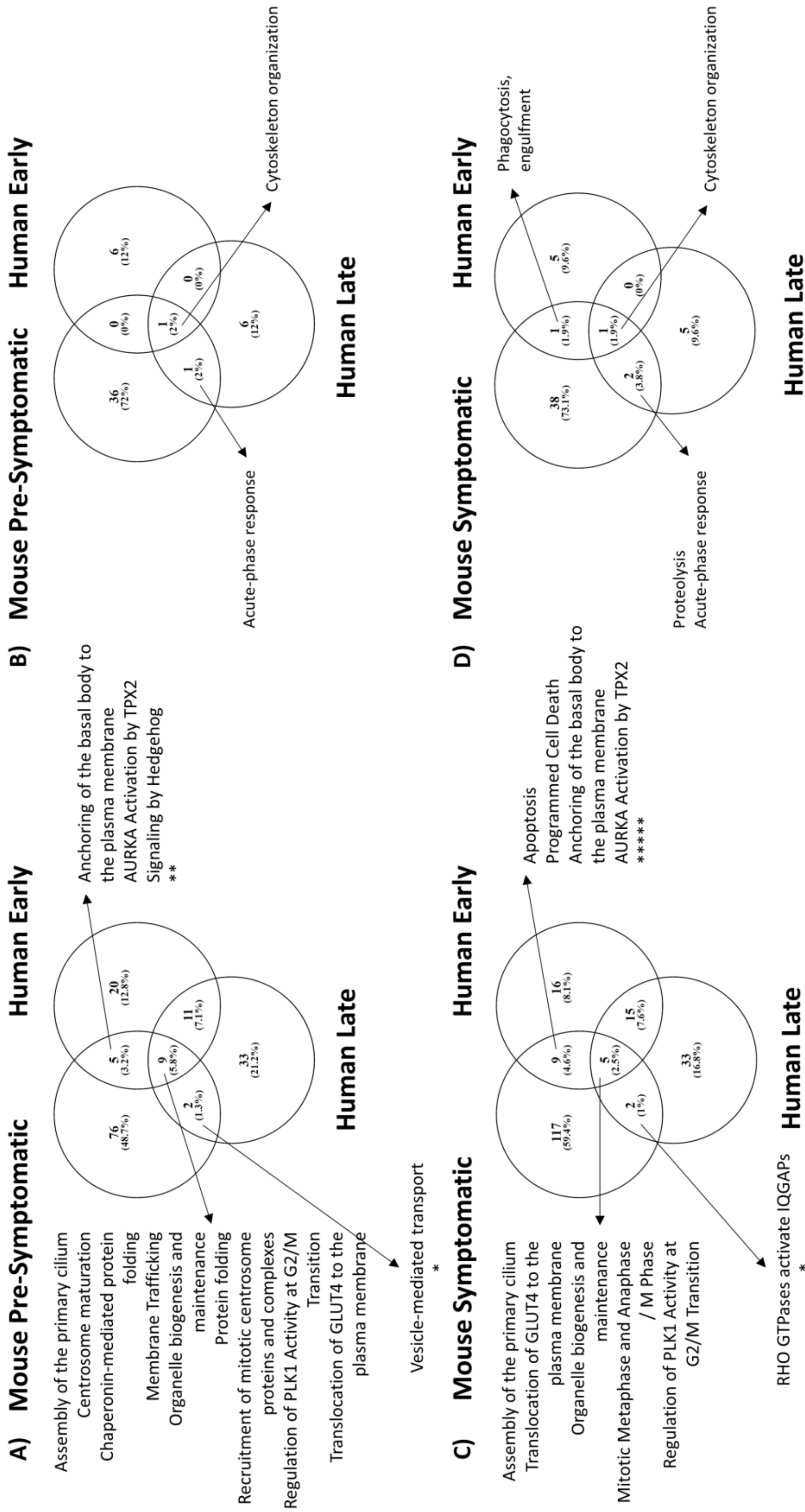

1031

1032 Figure 5

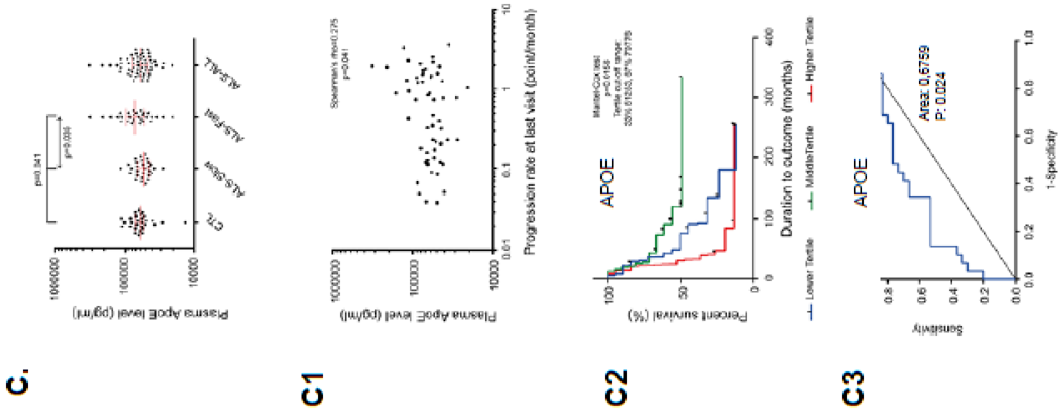

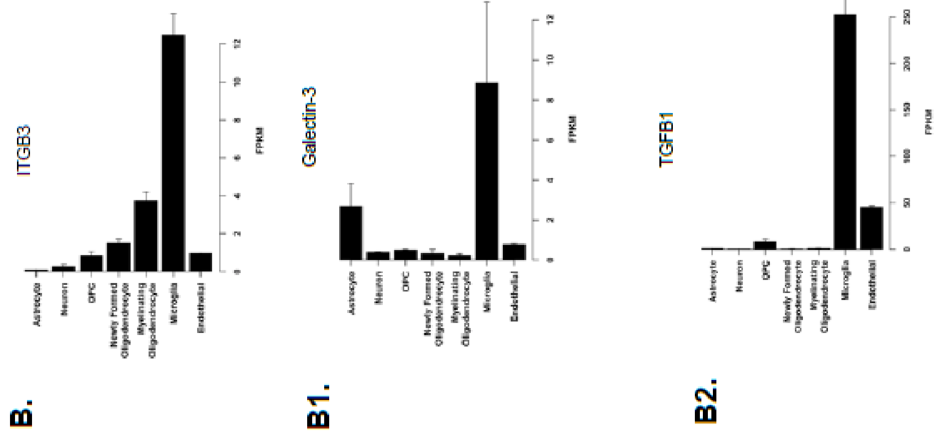

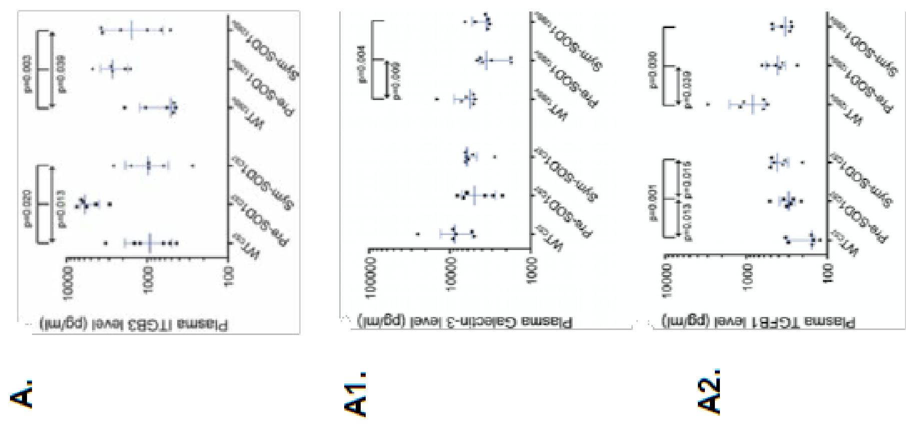

1033